Title:

Development of Novel Radioiodinated Exendin-4 Derivatives Targeting GLP-1 Receptor for Detection of β-cell Mass

Authors:

Yu Ogawa[1#], Hiroyuki Kimura[1,2#*], Hiroyuki Fujimoto[3], Hidekazu Kawashima[1,4], Kentaro Toyoda[3], Eri Mukai[3], Yusuke Yagi[1,2], Masahiro Ono[1], Nobuya Inagaki[3], and Hideo Saji[1*]

Affiliations:

[1]Department of Patho-Functional Bioanalysis, Kyoto University Graduate School of Pharmaceutical Sciences, 46-29, Yoshida Shimoadachi-cho, Sakyo-ku, Kyoto 606-8501, Japan

[2]Department of Analytical and Bioinorganic Chemistry, Kyoto Pharmaceutical University, 5 Nakauchi-cho, Misasagi, Yamashina-ku, Kyoto 607-8414, Japan

[3]Department of Diabetes, Endocrinology and Nutrition, Kyoto University Graduate School of Medicine, Kyoto University, 54 Shogoin Kawahara-cho, Sakyo-ku, Kyoto 606-8507, Japan

[4]Radioisotope Research Center, Kyoto Pharmaceutical University, 1 Misasagi-shichono-cho, Yamashina-ku, Kyoto 607-8412, Japan

*Hideo Saji, PhD

Department of Patho-Functional Bioanalysis, Kyoto University Graduate School of Pharmaceutical Sciences, 46-29, Yoshida Shimoadachi-cho, Sakyo-ku, Kyoto 606-8501, Japan

Phone: +81-75-753-4566; Fax: +81-75-753-4568; E-mail: hsaji@pharm.kyoto-u.ac.jp

*Hiroyuki Kimura, PhD

Department of Analytical and Bioinorganic Chemistry, Kyoto Pharmaceutical University, 5 Nakauchi-cho, Misasagi, Yamashina-ku, Kyoto 607-8414, Japan

E-mail: hkimura@mb.kyoto-phu.ac.jp

First Author: Yu Ogawa;

Department of Patho-Functional Bioanalysis, Kyoto University Graduate School of Pharmaceutical Sciences, 46-29, Yoshida Shimoadachi-cho, Sakyo-ku, Kyoto 606-8501, Japan

E-mail: y.ogawa_SKY1@hotmail.com, Phone: +81-75-753-4566; Fax: +81-75-753-4568

#Contributed equally to this work

Abstract

In subjects with type 2 diabetes mellitus (T2DM), pancreatic β-cell mass decreases; however, it is unknown to what extent this decrease contributes to the pathophysiology of T2DM. Therefore, the development of a method for noninvasive detection of β-cell mass is underway. We previously reported that glucagon-like peptide-1 receptor (GLP-1R) is a promising target molecule for β-cell imaging. In this study, we attempted to develop a probe targeting GLP-1R for β-cell imaging using single-photon emission computed tomography (SPECT). For this purpose, we selected exendin-4 as the lead compound and radiolabeled lysine at residue 12 in exendin-4 or additional lysine at the *C*-terminus using [^{123}I]iodobenzoylation. To evaluate *in vitro* receptor specificity, binding assay was performed using dispersed mouse islet cells. Biodistribution study was performed in normal ddY mice. *Ex vivo* autoradiography was performed in transgenic mice expressing green fluorescent protein under control of the mouse insulin I gene promoter. Additionally, SPECT imaging was performed in normal ddY mice. The affinity of novel synthesized derivatives toward pancreatic β-cells was not affected by iodobenzoylation. The derivatives accumulated in the pancreas after intravenous administration specifically via GLP-1R expressed on the pancreatic β-cells. Extremely high signal-to-noise ratio was observed during evaluation of biodistribution of [^{123}I]IB12-Ex4. SPECT images using normal mice showed that [^{123}I]IB12-Ex4 accumulated in the pancreas with high contrast between the pancreas and background. These results indicate that [^{123}I]IB12-Ex4 for SPECT is useful for clinical applications because of its preferable kinetics *in vivo*.

Keywords: glucagon-like peptide-1 receptor; exendin-4; β-cell imaging probe; ^{123}I

Introduction

In individuals with type 2 diabetes mellitus (T2DM), it is thought that loss of pancreatic β-cell mass (BCM) is as important as the decrease in function of each β cell[1-4]. We can estimate total β-cell function from clinical laboratory tests such as the homeostasis model assessment of β-cell function (HOMA-β) and insulinogenic index. BCM can be estimated by biopsy and autopsy studies; however, these are limited to cross-sectional information. Longitudinal information on BCM will enable us to understand the pathophysiology of diabetes more deeply. Therefore, noninvasive methods to evaluate BCM are currently under investigation.

Glucagon-like peptide-1 (GLP-1) is secreted from intestinal L cells, and it promotes insulin secretion in a glucose-dependent manner by binding to the GLP-1 receptor (GLP-1R)[5]. GLP-1R is highly expressed on pancreatic β cells and large ducts[6, 7]. GLP-1R agonists have already been used clinically for the treatment of T2DM[8, 9], and GLP-1R is a promising target to visualize pancreatic β cells and insulinomas[10]. We previously reported the potential of [^{125}I]BH-Ex(9-39) as a visualizing agent for pancreatic β cells[11]. We also have reported that ^{111}Indium (^{111}In)-labeled exendin-4 specifically accumulates in islet cells and that single-photon emission computed tomography (SPECT) with ^{111}In-labeled exendin-4 enables visualization of β cells *in vivo*[12-15]. Currently, ^{111}In, ^{68}Ga and ^{18}F-labeled exendin-4 has been widely investigated for visualization of pancreatic β cells and detection of insulinoma[10, 16-17]. However, few papers on radioiodinated exendin-4 have been reported yet[18-19].

In this study, we developed two radioiodinated exendin-4 derivatives thought to improve affinity to GLP-1R. Exendin-4 was labeled with *N*-succinimidyl-3-[^{123}I]iodobenzoate ([^{123}I]SIB) because it allowed easy synthesis of [^{123}I]iodobenzoylated ([^{123}I]IB) derivatives of peptides under mild conditions without exposure to oxidants[20, 21]. Finally, we evaluated the potential of two novel

synthesized [^{123}I]IB derivatives of exendin-4 ([^{123}I]IB-Ex4) as probes for detection of pancreatic β cells by SPECT.

Experimental Section

General

All reagents were purchased from Nacalai Tesque, Inc. (Kyoto, Japan) or FUJIFILM Wako Pure Chemical Corporation (Tokyo, Japan) and used without further purification unless otherwise noted. Ammonium [^{123}I]iodide ([^{123}I]NH_4I) (carrier free) solution was obtained from Nihon Medi-Physics Co., Ltd. (Tokyo, Japan). Because the half-life is long and handling is easy, ^{125}I instead of ^{123}I was used for biodistribution studies and *ex vivo* autoradiographic experiments. Sodium [^{125}I]iodide ([^{125}I]NaI) (carrier free) solution was purchased from MP Bio Japan K.K. (Tokyo, Japan). [^{125}I]BH-Ex(9-39) was purchased from PerkinElmer, Inc. (Waltham, MA, USA). Iodobenzoyl-modified exendin-4 derivatives and 9-fluorenylmethyl carbamate (Fmoc)-protected exendin-4 derivatives as precursors for radiolabeling were purchased from KNC Laboratories Co., Ltd. (Kobe, Japan) (Figure S1). The high-performance liquid chromatography (HPLC) system (Shimadzu, Kyoto, Japan) equipped with a US-3000 radio-HPLC detector (Universal Giken Co., Ltd., Odawara, Japan) was used for measuring purity.

Animals

Mice on a ddY background were obtained from Japan SLC, Inc. (Shizuoka, Japan). Transgenic mice expressing green fluorescent protein (GFP) under the control of mouse insulin promoter I

(MIP-GFP mice)[22] were maintained on an ICR background. Animal care and experimental procedures were approved by the Animal Care Committee of Kyoto University.

Radiosynthesis of Radioiodinated Exendin-4 Derivatives

Radiolabeled exendin-4 derivatives were synthesized according to the scheme presented in Fig. 1A and 1B. Precursor peptide (0.5 mg) in acetonitrile/buffer (50 mM borate, pH 7.8, containing 50 mM potassium chloride) (60:40, 100 μL) was added to acetonitrile containing [$^{123/125}$I]SIB[20]. Acetonitrile/triethylamine (98:2) was added stepwise until the pH reached 9.0. The reaction mixture was incubated at room temperature for an adequate time corresponding to the site of iodobenzoylation (Fig. 1C). Synthesized Fmoc-protected [$^{123/125}$I]IB12/40-Ex4 molecules were purified using HPLC. Piperidine (30 μL) was added to the resulting solution (500 μL). The reaction mixture was incubated at room temperature for 60 min. Synthesized [$^{123/125}$I]IB12/40-Ex4 were purified using HPLC. The radiochemical purities of labeled compounds were determined by analytical HPLC (Figure S2).

A

Compound Name	Structure
GLP-1(7-36)amide	H-HAEGTFTSDVSSYLEGQAAKEFIAWLVKGR-NH_2
Exendin-4	H-HGEGTFTSDLSKQMEEEAVRLFIEWLKNGGPSSGAPPPS-NH_2
Exendin(9-39)	H-DLSKQMEEEAVRLFIEWLKNGGPSSGAPPPS-NH_2
[*I]IB12-Ex4	H-HGEGTFTSDLSK([*I]IB)QMEEEAVRLFIEWLKNGGPSSGAPPPS-NH_2
[*I]IB40-Ex4	H-HGEGTFTSDLSKQMEEEAVRLFIEWLKNGGPSSGAPPPSK([*I]IB)-NH_2
Pre12-Ex4	Fmoc-HGEGTFTSDLSKQMEEEAVRLFIEWLK(Fmoc)NGGPSSGAPPPS-NH_2
Pre40-Ex4	Fmoc-HGEGTFTSDLSK(Fmoc)QMEEEAVRLFIEWLK(Fmoc)NGGPSSGAPPPSK-NH_2

B

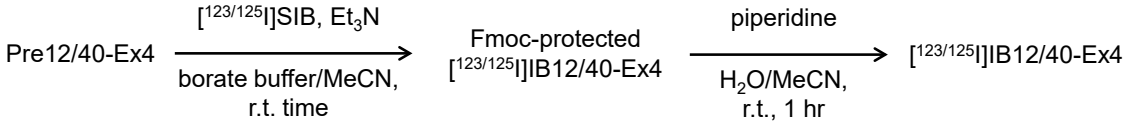

C

Compound	Time for iodobenzoylation (min)	Radiochemical yield (%)	Radiochemical purity (%)
[*I]IB12-Ex4	120	18.4	96
[*I]IB40-Ex4	30	28.3	> 99

FIGURE 1. Radiolabeled peptides were designed to detect pancreatic GLP-1R on β cells as a SPECT probe. (**A**) Primary structures of peptides. $^{123/125}$I in radiolabeled derivatives is shown in [*I]I. Pre12-Ex4 and Pre40-Ex4 are the precursor peptides for radiosynthesis of [*I]IB12-Ex4 and [*I]IB40-Ex4, respectively. (**B**) Synthetic scheme for radiosynthesis of [*I]IB-Ex4. (**C**) Radiosynthesis of [*I]IB-Ex4.

Radioligand Assays of Competitive Binding to Pancreatic Islets

Pancreatic islets dispersed as previously described and subjected to this competitive binding assay were used to assess the displacing effect of exendin(9-39) on GLP-1R binding[11, 23]. A collagenase digestion technique was used to isolate the pancreatic islets from male mice (ddY, 6 weeks old)[24]. A mixture of 0.05% Trypsin-EDTA (1×) and Phenol Red (Thermo Fisher Scientific,

Waltham, MA, USA)/phosphate-buffered saline (PBS) (pH 7.4, containing 0.53 mM EDTA) (20:80) was used to disperse the isolated islets. Islets were incubated with [^{125}I]BH-Ex(9-39) (3.7 kBq) in buffer (1 mL, 20 mM HEPES, pH 7.4, containing 1 mM magnesium chloride, 1 mg/mL bacitracin, and 1 mg/mL BSA) for 1 h at room temperature in the presence of varying concentrations of non-radiolabeled IB12/40-Ex4. Binding was terminated by rapid filtration through Whatman GF/C filters (24 mm), followed by washing thrice with 5 mL ice-cold PBS. Radioactivity of the filters was measured using an automatic γ-counter Wallac 1480 WIZARD 3" (PerkinElmer, Inc.). Specific binding was calculated as the difference between the total binding amount of [^{125}I]BH-Ex(9-39) and nonspecific binding. An inhibition curve and IC_{50} against [^{125}I]BH-Ex(9-39) was determined by statistical analysis using GraphPad Prism software (version 5.03 for Windows; GraphPad, Inc., San Diego, CA, USA). Data are means ± SEM (n = 4 per group).

Biodistribution Studies

For biodistribution studies of [^{125}I]IB12/40-Ex4, male mice (ddY, 6 weeks old) were used. [^{125}I]IB12/40-Ex4 in saline (0.1 mL/dose, 18.5 kBq/mL) was administered to the mice via tail vein injection. At 5, 15, 30, 60, and 120 min after administration, the mice were euthanized by exsanguination.

For *in vivo* blocking studies of [^{125}I]IB12-Ex4, exendin(9-39) in saline (0.1 mL/dose, 500 μg/mL) was preliminarily administered to the mice via tail vein injection 30 min before the administration of [^{125}I]IB12-Ex4[11]. At 30 min after the administration of [^{125}I]IB12-Ex4, the mice were euthanized by exsanguination.

Blood and organs were harvested from the mice and weighed. The automatic γ-counter Wallac 1480 WIZARD 3" was used to measure the radioactivity in the blood and organs. Radioactivity levels were expressed as %ID/g. Data are means ± SD (n = 5 per group).

Ex vivo Autoradiographic Experiments

[^{125}I]IB12-Ex4 in saline (0.1 mL/dose, 1.85 MBq/mL) was administered to male MIP-GFP mice via tail vein injection. At 30 min after administration, the mice were euthanized by exsanguination. The pancreases were harvested and cut into several pieces. Each piece was placed on a glass slide and pressed with a cover glass. An image analyzer Typhoon 9410 (GE Healthcare, Milwaukee, WI, USA) was used to evaluate the fluorescence and radioactivity signals in the pancreatic sections. Fluorescence emission at 520 nm from the pancreatic sections with excitation at 457 nm was detected. Autoradiograms were obtained from imaging plates exposed to the pancreatic section for 18 h.

For *in vivo* blocking studies, exendin(9-39) in saline (0.1 mL/dose, 500 μg/mL) was preliminarily administered to the mice via tail vein injection 30 min before the administration of [^{125}I]IB12-Ex4[11]. After 30 min, mice were euthanized by exsanguination. Pancreases were harvested and handled using the same method as that used for the control.

SPECT/Computed Tomography (CT) Acquisition and Processing

In SPECT/CT studies, male mice (ddY, 6 weeks old) were used. A pre-clinical imaging system Triumph LabPET12/SPECT4/CT scanner (TriFoil Imaging Inc., Chatsworth, CA, USA) was used to acquire and process the SPECT and CT data. A nanoparticle CT contrast agent ExiTron nano

6000 (Miltenyi Biotec, Bergisch Gladbach, Germany) (0.1 mL/dose) was administered via tail vein injection 4 h before administration of [^{123}I]IB12-Ex4. [^{123}I]IB12-Ex4 in saline (0.15 mL/dose, 94.0 MBq/mL) was administered to the mice via tail vein. At 30 min after administration, the mice were anesthetized with isoflurane (2.0% isoflurane), and a four-head detector camera was used to perform tomographic spiral SPECT scans of the anesthetized mice.

A modified 3D cone-beam Feldkamp algorithm was used to reconstruct the CT projections. The SPECT projection data were processed to create a quantitative image. A 20% energy window centered on 159 keV was used for ^{123}I acquisitions. A 3D-ordered subsets-expectation maximization algorithm (5 iterations, 8 subsets) resulting in an 80 × 80 × 80 image matrix with a 0.835 × 0.826 × 0.598 mm voxel size was used to reconstruct the SPECT projections. Amira 3D data analysis and visualization software (version 5.1; FEI Company, Hillsboro, OR, USA) was used to perform image analysis.

Statistical Analysis

GraphPad Prism (version 5.03 for Windows; GraphPad Software, San Diego, CA, USA) was used to perform statistical analysis. Student's *t*-test was used to compare the blood and organ uptake ratios of [^{125}I]IB12-Ex4 with those of [^{125}I]IB40-Ex4 and to compare the tissue uptake of the control mice with those of the blocked mice in the biodistribution studies. The statistical significance level was set at $p < 0.05$.

Results

Radiosynthesis of Radioiodinated Exendin-4 Derivatives

Structures of designed peptides are shown in Fig. 1A. The peptides Pre12-Ex4 and Pre40-Ex4 were designed as precursor for [$^{123/125}$I]IB12-Ex4 and [$^{123/125}$I]IB40-Ex4, respectively. A synthetic scheme for radiolabeling is shown in Fig. 1B. Radiochemical yields based on [$^{123/125}$I]SIB and radiochemical purities are shown in Fig. 1C. Both derivatives were synthesized with sufficient quantities and purity for use as imaging agents for SPECT.

In Vitro Biding Assays

The binding of [^{125}I]BH-Ex(9-39) to islets of mice was inhibited by exendin-4; [^{125}I]BH-Ex(9-39) and exendin-4 bound competitively to pancreatic GLP-1R. The assay showed that similar to exendin-4, IB12/40-Ex4 also inhibited the binding of [^{125}I]BH-Ex(9-39) in a concentration-dependent manner (Fig. 2A). The 50% inhibitory concentration (IC_{50}) values of IB12-Ex4 and IB40-Ex4 were 3.37 and 1.97 nM, respectively, which revealed that both derivatives had high affinity for GLP-1R similar to that of exendin-4 (Fig. 2B).

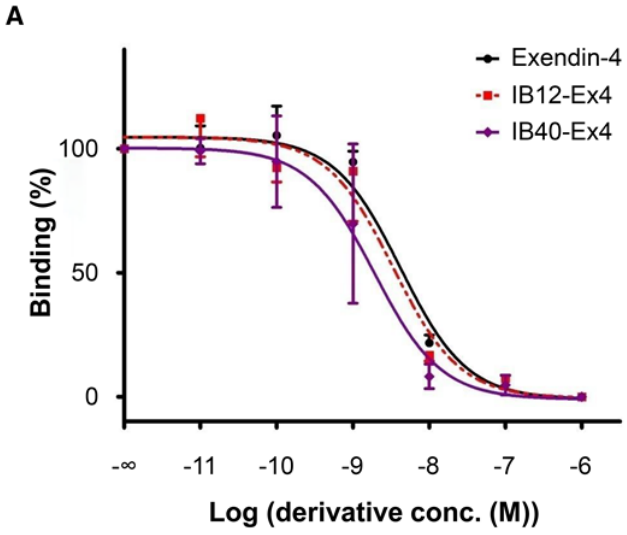

B

Compound	IC_{50} (nM)
Exendin-4	4.20 (2.30 - 7.69)
IB12-Ex4	3.37 (1.23 - 8.77)
IB40-Ex4	1.92 (0.998 - 3.71)

FIGURE 2. Inhibitory activity of IB-Ex4 on [^{125}I]BH-Ex(9-39) binding to pancreatic islets. (**A**) Specific binding of [^{125}I]BH-Ex(9-39) and displacement curves. Data are means ± SEM (n = 4 per

group). (**B**) Best-fit values and 95% confidence intervals of 50% inhibitory concentration obtained from this assay. R squares were > 0.85 in experiments performed to examine binding specificity of each compound.

Biodistribution Studies of ddY Mice

Radioactivity in selected organs was measured after intravenous administration of [^{125}I]IB12-Ex4 or [^{125}I]IB40-Ex4 (Fig. 3A and 3B). The highest value of radioactivity level in the pancreas was 43.66 ± 2.28% of the injected dose per gram (%ID/g) at 30 min after injection of [^{125}I]IB12-Ex4.

We calculated the ratio of the radioactivity level in the pancreas to that in the blood, stomach, intestine, liver, and spleen to evaluate the signal-to-noise (S/N) ratio (Fig. 3C). The pancreas-to-blood (P/B) and pancreas-to-spleen (P/Sp) ratios were higher for [^{125}I]IB12-Ex4 than for [^{125}I]IB40-Ex4 at each time point. The pancreas-to-liver (P/L) ratio was higher for [^{125}I]IB12-Ex4 than for [^{125}I]IB40-Ex4 at each time point, except at 120 min. The pancreas-to-stomach (P/St) ratio neither increased nor decreased with time. The pancreas-to-intestine (P/I) ratio was higher for [^{125}I]IB12-Ex4 than for [^{125}I]IB40-Ex4 until 15 min after injection, when the P/I ratios of both compounds decreased similarly. Compared with other previously reported imaging probes targeting β-cell proteins, these ratios were significantly higher[11, 18].

A

Biodistribution of [^{125}I]IB12-Ex4 in mice					
Time after injection (min)	**5**	**15**	**30**	**60**	**120**
Pancreas	25.77±2.26	35.35±2.75	43.66±2.28	34.15±3.19	22.91±3.61
Blood	5.41±0.57	3.06±0.35	2.20±0.19	1.54±0.15	0.76±0.15
Heart	3.28±0.37	2.28±0.56	1.88±0.45	1.98±0.42	0.70±0.16
Lung	94.71±21.37	115.99±16.69	143.73±22.25	136.51±14.39	84.62±14.52
Stomach	4.19±1.83	5.88±3.43	7.18±1.43	5.17±0.50	3.71±2.04
Intestine	2.97±0.47	3.70±0.70	5.67±1.11	6.02±0.37	6.28±1.59
Liver	2.45±0.18	3.15±0.35	2.92±0.48	2.30±0.17	1.36±0.24
Spleen	2.11±0.35	1.52±0.21	1.14±0.24	0.86±0.18	0.43±0.09
Kidney	38.22±4.84	33.34±1.53	21.31±2.87	13.88±0.90	8.32±1.89
Thyroid	5.33±0.81	3.80±0.98	4.02±0.93	2.58±0.74	3.32±1.94

B

Biodistribution of [^{125}I]IB40-Ex4 in mice					
Time after injection (min)	**5**	**15**	**30**	**60**	**120**
Pancreas	7.40±1.86	16.20±2.16	26.13±4.95	26.50±1.58	24.15±4.53
Blood	31.73±1.85	23.63±2.45	16.26±2.40	10.46±0.84	6.08±1.19
Heart	6.72±0.64	6.24±1.02	5.42±1.13	3.47±0.22	2.34±0.42
Lung	30.76±2.05	44.55±12.17	55.33±13.48	55.93±14.15	52.08±10.84
Stomach	2.15±0.28	2.67±0.74	4.12±1.64	6.97±0.62	5.35±0.71
Intestine	2.64±0.45	2.64±0.67	3.33±0.52	4.26±0.47	5.64±2.24
Liver	6.79±1.12	5.78±0.63	3.93±0.53	3.09±0.44	2.04±0.46
Spleen	5.26±0.27	4.80±0.79	3.70±0.71	2.20±0.22	2.20±0.32
Kidney	14.27±1.33	18.90±2.28	14.94±2.82	11.02±1.19	9.65±2.59
Thyroid	7.06±1.33	8.07±2.08	4.96±1.26	2.88±0.54	2.71±1.33

C

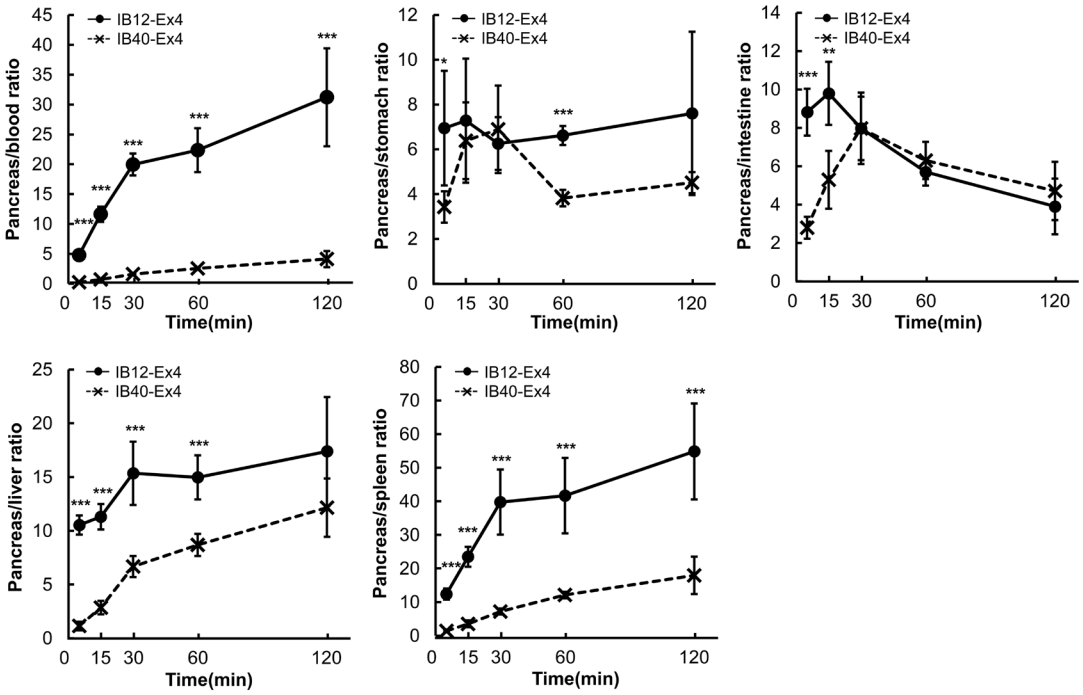

FIGURE 3. *In vivo* biodistribution of [^{125}I]IB12/40-Ex4 in normal mice. (**A**) Biodistribution of [^{125}I]IB12-Ex4. (**B**) Biodistribution of [^{125}I]IB40-Ex4. Data are means ± SD (n = 5 per group). (**C**) Uptake ratio of pancreas-to-blood or organs in the proximity to the pancreas. Ratios were calculated based on %ID/g of each organ. P/B, P/St, P/I, P/L, and P/Sp ratios of [^{125}I]IB12/40-Ex4 are shown. *p < 0.05, **p < 0.01, and ***p < 0.001 compared with the uptake ratio of [^{125}I]IB40-Ex4 at the same time points. Organs are denoted as follows: P, pancreas; B, blood; St, stomach; I, intestines; L, liver; Sp, spleen.

Specific Accumulation of Radioiodinated Exendin-4 Derivatives at Pancreatic β-cells via GLP-1R

We confirmed the localization of radioactivity in the pancreas using transgenic mice expressing GFP under the control of mouse insulin promoter I (MIP-GFP mice)[11, 22]. Sections of pancreases harvested from MIP-GFP mice injected with [^{125}I]IB12-Ex4 were assessed for fluorescent and radioactive signals. Detected radioactive signals colocalized well with the fluorescent signals (Fig. 4A), indicating that [^{125}I]IB12-Ex4 accumulates in pancreatic β cells. To confirm specific binding to GLP-1R, we conducted a biodistribution study with the inhibition of GLP-1R. The radioactivity at 30 min after injection of excess exendin(9-39) showed a dramatic decrease in the pancreas and lungs, where GLP-1R is highly expressed[25]. Pancreata from mice with GLP-1R inhibition reached only 4.8% of the radioactivity of those of control mice (Fig. 4B). Similarly, radioactive signals in the pancreatic β cells of MIP-GFP mice disappeared with inhibition.

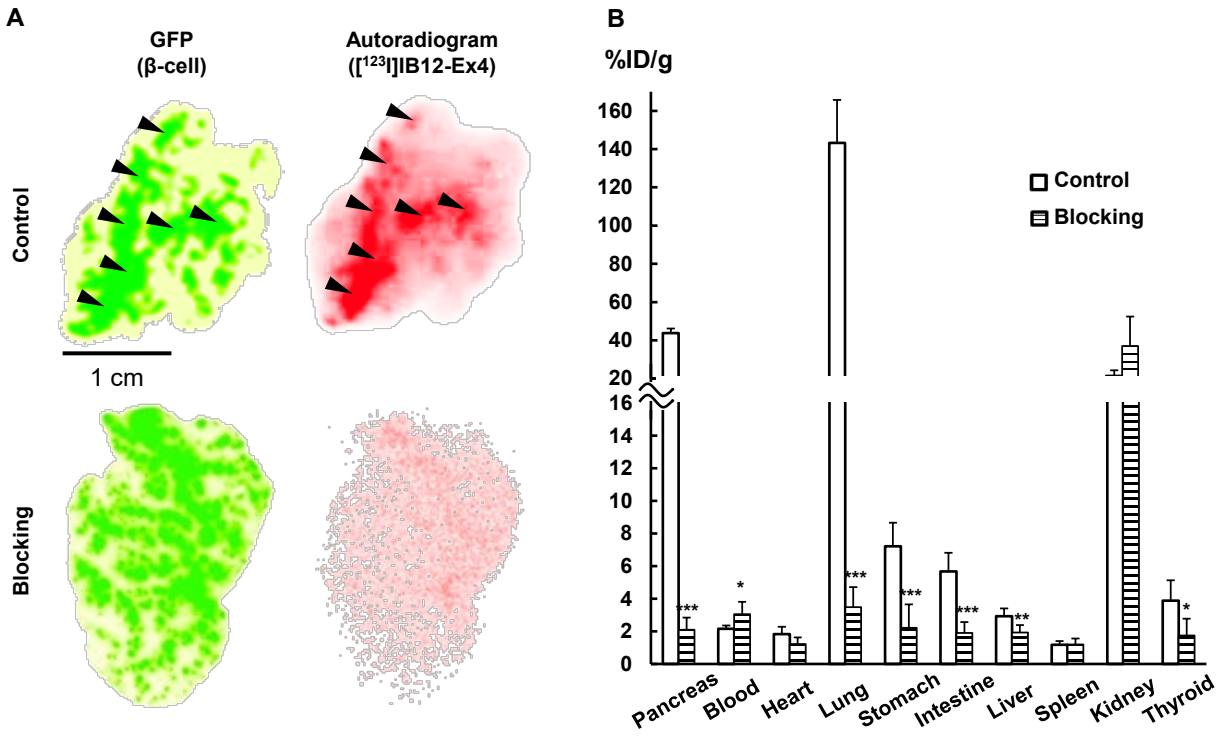

FIGURE 4. Radioactivity in the pancreas binds to β-cells via GLP-1R. (**A**) Comparison of the fluorescence image with the autoradiogram of pancreatic sections harvested from MIP-GFP mice (n =3). GFP shows the distribution of β-cells. Autoradiogram shows the distribution of [^{125}I]IB12-Ex4. Corresponding spots in control images were shown with black arrowheads. Bar = 1 cm. (**B**) *In vivo* biodistribution of [^{125}I]IB12-Ex4 in mice pretreated with excess exendin(9-39). Data are means ± SD (n = 5 per group). In the pancreas, 41.7%ID/g of the accumulation was reduced by blocking. This value was 95.2% of the accumulation in the pancreas of control mice. *$p < 0.05$, **$p < 0.01$, ***$p < 0.001$ compared with the uptake in control mice.

SPECT/CT Studies of ddY Mice

We performed SPECT acquisition of ddY mice injected with [^{123}I]IB12-Ex4 to evaluate the actual SPECT image. After SPECT acquisition, X-ray CT was performed with a contrast agent

that provides strong contrast for visualizing liver and spleen[26]. Visualizing the morphology of the liver and spleen in the CT image enables clear visualization of the radioactivity in the pancreas on the SPECT image[13]. Thus, the radioactivity in the pancreas was clearly visualized on the SPECT image (Fig. 5A–C).

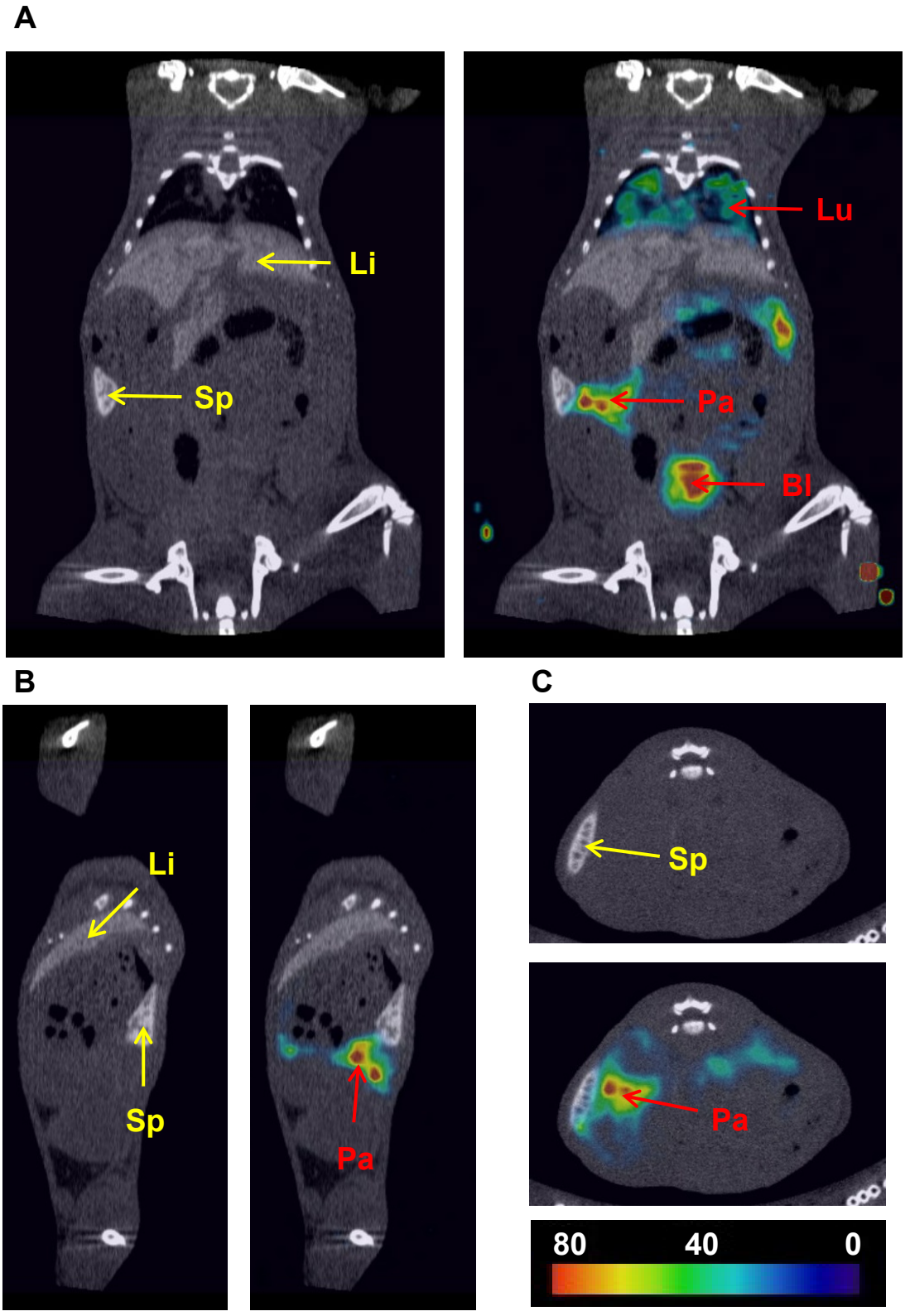
A
Li
Sp
Lu
Pa
Bl
B
Li
Sp
Pa
C
Sp
Pa
80
40
0

FIGURE 5. The SPECT images of normal mice injected [^{123}I]IB12-Ex4. SPECT images showed high radioactivity in the pancreas. (**A**) CT and SPECT/CT fusion image of coronal cross section including pancreas (dorsal view). (**B**) CT and SPECT/CT fusion image of sagittal cross section including pancreas (left lateral view). In CT images, liver (Li) and spleen (Sp) were provided strong contrast by contrast agent. In SPECT/CT fusion images high density of radioactivity was found in pancreas (Pa), lung (Lu) and bladder (Bl). (**C**) CT and SPECT/CT fusion image of transverse cross section including pancreas (caudal view).

Discussion

In this study, we aimed to develop a robust, noninvasive method for imaging pancreatic β cells. A designed probe must meet two requirements for clear imaging of the pancreas: (1) specific accumulation at pancreatic β cells and (2) a high uptake ratio in the pancreas compared with various proximal organs and the blood. Therefore, we focused on GLP-1R and designed a probe based on its ligand, exendin-4. Because the *N*-terminus of exendin-4 interacts with the extracellular surface of the receptor[27] and the amino group of Lys[27] is important for binding to GLP-1R[28], we designed only two derivatives, IB12-Ex4 and IB40-Ex4, whose lysine residues at 12 and 40 were labeled, respectively. We successfully synthesized radiolabeled IB12/40-Ex4, [^{123}I]IB12/40-Ex4, and IB12/40-Ex4 showed almost the same affinity as exendin-4 for GLP-1R, indicating that these two modifications did not affect the affinity of exendin-4 for GLP-1R.

In the biodistribution study, [^{125}I]IB12/40-Ex4 showed renal excretory kinetics similar to those of exendin-4. However, a significant difference was observed between the two derivatives: a slower clearance of radioactivity from the blood was observed for [^{125}I]IB40-Ex4 than for [^{125}I]IB12-Ex4. The reason for this could be that IB12-Ex4 tends to exist in free form in the blood.

Exendin-4 has been reported to be predominantly eliminated by renal mechanisms, particularly by glomerular filtration[29-31]. As the molecular weights of the two derivatives are < 5,000, a derivative existing in free form in the blood should be smoothly eliminated by glomerular filtration. This difference in the derivatives is probably owing to the difference in clearance. Indeed, our biodistribution studies also showed more rapid transfer of [^{125}I]IB12-Ex4 than that of [^{125}I]IB40-Ex4 to the kidney.

β cells reside in the islets, whose size ranges from 50 to 500 μm in diameter and are scattered throughout the pancreas. These β cells represent approximately 1%–2% of the pancreatic mass and occupy 50%–80% of each islet[32-34]. This distribution of β cells is most probably the underlying reason for the previous difficulties in the visualization of β cell proteins using macroscopic imaging techniques[35]. We demonstrate a SPECT image that distinctly visualizes the healthy pancreas. Ratios of P/B, P/St, P/I, P/L, P/Sp, and P/K calculated from mouse organs were similar to those obtained from the biodistribution study. Clear imaging achieved by our SPECT study demonstrates that the uptake ratios of [^{123}I]IB12-Ex4 are sufficient for distinct visualization of the pancreas.

Further development of our probe presented herein and readily available quantitative SPECT would allow a better understanding of the relationships between BCM and glucose homeostasis. Evaluation of the change in BCM to the level of T2DM should provide important information for the elucidation of the pathology of diabetes. Furthermore, because an up-to-date report implies that a decrease in BCM precedes impaired glucose tolerance[36], quantification of BCM has the potential to diagnose T2DM earlier than present diagnostic functional tests.

Conclusions

[^{123}I]IB12-Ex4 has shown many promising results in this study that merit its further development and application for various investigational aims in the field of diabetology.

Acknowledgments

Funding: This work was supported by the Practical Research for Innovative Cancer Control from the Japan Agency for Medical Research and Development (AMED) (17ck0106149h0003) and the Center of Innovation Program from MEXT and JST(201111005B). The authors declare no competing financial interests.

Conflict of Interest Disclosure: The authors declare no competing financial interest.

Associated Content

Supporting Information

Mass spectra, Radio-RP-HPLC chromatograms (MS Word)

References

1. Butler, A. E.; Janson, J.; Bonner-Weir, S.; et al. β-Cell Deficit and Increased β-Cell Apoptosis in Humans with Type 2 Diabetes. *Diabetes* **2003,** *52,* 102–110.

2. Sakuraba, H.; Mizukami, H.; Yagihashi, N.; et al. Reduced Beta-Cell Mass and Expression of Oxidative Stress-Related DNA Damage in the Islet of Japanese Type II Diabetic Patients. *Diabetologia* **2002,** *45,* 85–96.

3. Rahier, J.; Guiot, Y.; Goebbels, R. M.; et al. Pancreatic β-Cell Mass in European Subjects with type 2 Diabetes. *Diabetes Obes. Metab.* **2008,** *10,* 32–42.

4. Meier, J. J. Beta Cell Mass in Diabetes: A Realistic Therapeutic Target? *Diabetologia* **2008,** *51,* 703–713.

5. Holz, G. G.; Kühtreiber, W. M.; Habener, J. F. Pancreatic Beta-Cells Are Rendered Glucose-Competent by the Insulinotropic Hormone Glucagon-Like peptide-1(7-37). *Nature* **1993,** *361,* 362–365.

6. Dillon, J. S.; Tanizawa, Y.; Wheeler, M. B.; et al. Cloning and Functional Expression of the Human Glucagon-Like peptide-1 (GLP-1) Receptor. *Endocrinology* **1993,** *133,* 1907–1910.

7. Tornehave, D.; Kristensen, P.; Rømer, J.; et al. Expression of the GLP-1 Receptor in Mouse, Rat, and Human Pancreas. *J. Histochem. Cytochem.* **2008,** *56,* 841–851.

8. Chia, C. W.; Egan, J. M. Role and Development of GLP-1 Receptor Agonists in the Management of Diabetes. *Diabetes Metab. Syndr. Obes.* **2009,** *2,* 37.

9. Kruger, D. F.; Bode, B.; Spollett, G. R. Understanding GLP-1 Analogs and Enhancing Patient Success. *Diabetes Educ.* **2010,** *36,* 44S–72S; quiz 73S.

10. Wei, W.; Ehlerding, E. B.; Lan, X.; et al. Molecular Imaging of β-Cells: Diabetes and Beyond. *Adv. Drug Deliv. Rev.* **2019,** *139,* 16–31.

11. Mukai, E.; Toyoda, K.; Kimura, H.; et al. GLP-1 Receptor Antagonist as a Potential Probe for Pancreatic β-Cell Imaging. *Biochem. Biophys. Res. Commun.* **2009,** *389,* 523–526.

12. Kimura, H.; Fujita, N.; Kanbe, K.; et al. Synthesis and Biological Evaluation of an ^{111}In-Labeled exendin-4 Derivative as a Single-Photon Emission Computed Tomography Probe for Imaging Pancreatic β-Cells. *Bioorg. Med. Chem.* **2017,** *25,* 5772–5778.

13. Hamamatsu, K.; Fujimoto, H.; Fujita, N.; et al. Establishment of a Method for In-Vivo SPECT/CT Imaging Analysis of ^{111}In-Labeled exendin-4 Pancreatic Uptake in Mice Without the Need for Nephrectomy or a Secondary Probe. *Nucl. Med. Biol.* **2018,** *64–65,* 22–27.

14. Fujita, N.; Fujimoto, H.; Hamamatsu, K.; et al. Non-Invasive Longitudinal Quantification of Beta Cell Mass with ^{111}Indium-Labeled exendin-4. *F.A.S.E.B. J.* **2019**, 33, 11836–11844.

15. Murakami, T.; Fujimoto, H.; Fujita, N.; et al. Noninvasive Evaluation of GPR119 Agonist Effects on β-Cell Mass in Diabetic Male Mice Using ^{111}In-Exendin-4 SPECT/CT. *Endocrinology*. **2019**, *160*, 2959–2968.

16. Jodal, A.; Schibli, R.; Béhé, M.; Targets and probes for non-invasive imaging of β-cells. *Eur J Nucl Med Mol Imaging*, **2017**, *44*, 712–727

17. Jansen, T. J. P.; Lith, S. A. M.; Boss, M; et al. Exendin-4 Analogs in Insulinoma Theranostics. *J Label Compd Radiopharm.* **2019**, *62*, 656–672.

18. Lappchen, T.; Tonnesmann, R.; Eersels, J.; et al. Radioiodinated Exendin-4 Is Superior to the Radiometal-Labelled Glucagon-Like Peptide-1 Receptor Probes Overcoming Their High Kidney Uptake *PLOS ONE.* **2017,** 12(1), e0170435.

19. Eriksson, O.; Korsgren, O.;Selvaraju, R. K.; .; et al. Pancreatic Imaging Using an Antibody Fagment Targeting the Zinc Transporter Type 8: a Direct Comparison with Radio-Iodinated Exendin-4. *Acta Diabetol.* **2018,** *55,* 49–57.

20. Zalutsky, M. R.; Narula, A. S. A Method for the Radiohalogenation of Proteins Resulting in Decreased Thyroid Uptake of Radioiodine. *Appl. Radiat. Isot.* **1987,** *38,* 1051–1055.

21. Al-Jammaz, I.; Al-Otaibi, B.; Amartey, J. K. A Novel Route to Radioiodinated [^{123}I] −*N*-succinimidyl-3-iodobenzoate, a Reagent for Radioiodination of Bioactive Peptides. *Appl. Radiat. Isot.* **2002,** *57,* 743–747.

22. Hara, M.; Wang, X.; Kawamura, T.; et al. Transgenic Mice with Green Fluorescent Protein-Labeled Pancreatic β-Cells. *Am. J. Physiol. Endocrinol. Metab.* **2003,** *284,* E177–E183.

23. Mukai, E.; Ishida, H.; Kato, S.; et al. Metabolic Inhibition Impairs ATP-Sensitive K^+ Channel Block by Sulfonylurea in Pancreatic β-Cells. *Am. J. Physiol.*; Simpson **1998,** *274,* E38–E44.

24. Sutton, R.; Peters, M.; McShane, P.; et al. Isolation of Rat Pancreatic Islets by Ductal Injection of collagenase1. *Transplantation* **1986,** *42,* 689–691.

25. Vahl, T. P.; Tauchi, M.; Durler, T. S.; et al. Glucagon-Like Peptide-1 (GLP-1) Receptors Expressed on Nerve Terminals in the Portal Vein Mediate the Effects of Endogenous GLP-1 on Glucose Tolerance in Rats. *Endocrinology* **2007,** *148,* 4965–4973.

26. Boll, H.; Nittka, S.; Doyon, F.; et al. Micro-CT Based Experimental Liver Imaging Using a Nanoparticulate Contrast Agent: A Longitudinal Study in Mice. *PLOS ONE* **2011,** *6,* e25692.

27. Runge, S.; Schimmer, S.; Oschmann, J.; et al. Differential Structural Properties of GLP-1 and Exendin-4 Determine Their Relative Affinity for the GLP-1 Receptor N-Terminal Extracellular Domain. *Biochemistry* **2007,** *46,* 5830–5840.

28. Runge, S.; Thøgersen, H.; Madsen, K.; et al. Crystal Structure of the Ligand-Bound Glucagon-Like Peptide-1 Receptor Extracellular Domain. *J. Biol. Chem.* **2008,** *283,* 11340–11347.

29. Copley, K.; McCowen, K.; Hiles, R.; et al. Investigation of Exenatide Elimination and Its *In Vivo* and *In Vitro* Degradation. *Curr. Drug Metab.* **2006,** *7,* 367–374.

30. Simonsen, L.; Holst, J. J.; Deacon, C. F. Exendin-4, but Not Glucagon-Like peptide-1, Is Cleared Exclusively by Glomerular Filtration in Anaesthetised Pigs. *Diabetologia* **2006,** *49,* 706–712.

31. Linnebjerg, H.; Kothare, P. A.; Park, S.; et al. Effect of Renal Impairment on the Pharmacokinetics of Exenatide. *Br. J. Clin. Pharmacol.* **2007,** *64,* 317–327.

32. Saito, K.; Yaginuma, N.; Takahashi, T. Differential Volumetry of A, B and D Cells in the Pancreatic Islets of Diabetic and Nondiabetic Subjects. *Tohoku J. Exp. Med.* **1979,** *129,* 273–283.

33. Maffei, A.; Liu, Z.; Witkowski, P.; et al. Identification of Tissue-Restricted Transcripts in Human Islets. *Endocrinology* **2004,** *145,* 4513–4521.

34. Göke, B. Islet Cell Function: α and β Cells—Partners Towards Normoglycaemia. *Int. J. Clin. Pract.* **2008,** *62,* 2–7.

35. Brom, M.; Weg, W. W.; Joosten, L., et al. Non-Invasive Quantification of the Beta Cell Mass by SPECT with ^{111}In-Labeled Exendin. *Diabetologia* **2014,** *57,* 950–959.

36. Meier, J. J.; Breuer, T. G.; Bonadonna, R. C.; et al. Pancreatic Diabetes Mainfests When Beta Cell Area Declines by Approximately 65% in Humans. *Diabetologia* **2012,** *55,* 1346–1354.